Shear bands as manifestation of a criticality in yielding amorphous solids

Giorgio Parisi[a,1], Itamar Procaccia[b,1], Corrado Rainone[b], and Murari Singh[b]

[a]Dipartimento di Fisica, Sapienza Universitá di Roma, Istituto Nazionale di Fisica Nucleare, Sezione di Roma I, Istituto per i Processi Chimico-Fisici (IPCF)–Consiglio Nazionale delle Ricerche, I-00185 Rome, Italy; and [b]Department of Chemical Physics, The Weizmann Institute of Science, Rehovot 76100, Israel

Contributed by Giorgio Parisi, April 19, 2017 (sent for review February 6, 2017; reviewed by Antonio Coniglio and Olivier Dauchot)

Amorphous solids increase their stress as a function of an applied strain until a mechanical yield point whereupon the stress cannot increase anymore, afterward exhibiting a steady state with a constant mean stress. In stress-controlled experiments, the system simply breaks when pushed beyond this mean stress. The ubiquity of this phenomenon over a huge variety of amorphous solids calls for a generic theory that is free of microscopic details. Here, we offer such a theory: The mechanical yield is a thermodynamic phase transition, where yield occurs as a spinodal phenomenon. At the spinodal point, there exists a divergent correlation length that is associated with the system-spanning instabilities (also known as shear bands), which are typical to the mechanical yield. The theory, the order parameter used, and the correlation functions that exhibit the divergent correlation length are universal in nature and can be applied to any amorphous solids that undergo mechanical yield.

shear bands | yielding | glass | spinodal | criticality

A solid, be it crystalline or amorphous, is operatively defined as any material capable to respond elastically to an externally applied shear deformation (1). However, any solid material, when subject to a large-enough shear strain, finally undergoes a mechanical yield. Here, we focus on the mechanical yield of amorphous materials, such as molecular and colloidal glasses, foams, and granular matter. The phenomenology exhibited by the yielding point within this vast class of materials, as reported in countless strain-controlled simulations (2–8) and experiments (9–11), shows a remarkable degree of universality, despite the highly varied nature of the model systems involved. Among these universal features is the presence, at the onset of flow at yielding, of system-spanning excitations referred to as shear bands (12, 13), wherein the shear strongly localizes, leaving the rest of the material unperturbed. This phenomenon is of capital importance for engineering applications, because it is responsible for the brittleness typical of glassy materials, in particular metallic glasses (14), whose potential for practical use is stymied by their tendency to shear band and fracture (13, 15, 16).

In athermal amorphous solids, the phenomenon has universal features. For strains γ smaller than some critical value denoted as γ_Y, the stress in the material grows on the average when the strain is increased. After yield, the stress cannot grow on the average, no matter how much the strain is increased. The universality of the basic phenomenology of yielding begs a picture of its characteristics in terms of a universal theory, in the sense that such a theory should rely on a statistical–mechanical framework and be independent of details, such as chemical composition and production process of the material. This need was addressed in a recent work (17), wherein building up from ideas first advanced in ref. 18, there emerged a picture of mechanical yielding as a first-order phenomenon [i.e., as a discontinuous phase transition in a suitable overlap order parameter Q_{ab} (defined in Eq. **1** below), which jumps from a value of order one to a value of order zero as strain is increased above the yielding threshold γ_Y]. The physical meaning of this observation is that, before yielding, the amorphous system was limited to a small patch in the configuration space, very far from any kind of ergodicity. The yielding transition is an opening of a much larger available configuration space, whereupon the system is ergodized subject to the constraint of constant mean stress. Within this framework, the yielding transition is essentially envisioned as a spinodal point (19) (i.e., the point where the metastable, high-Q_{ab} glassy patch of available configurations becomes unstable with respect to a new phase with low Q_{ab}) associated with an ergodized system in the presence of disorder (20). A paradigmatic example of such a spinodal is the mode coupling cross-over (12) characterized by dynamical slowing down and heterogeneities, with behavior that is characterized by a dynamical length scale, which can be extracted from suitable multipoint correlators (12). According to our picture, this kind of critical behavior should also be found at the yielding transition, conditional that one is able to derive the expression of the right correlator to measure. This suggestion seems even more reasonable in light of a recent study (21), wherein the similarity of shear bands with dynamical heterogeneities has been pointed out; also, some oscillatory shear simulations seem to indicate that a slowdown of the dynamics on approaching yielding may indeed be present (22, 23). It is important to stress here that the reason that a spinodal point can be exposed and measured is that the glassy timescales and the athermal conditions stabilize the metastable system until the spinodal point is crossed and the system becomes unstable against constrained ergodization.

Within a generic statistical–mechanical theory, formulated in terms of a suitable Gibbs free energy $G[\phi]$ (i.e., the free energy for fixed order parameter ϕ), stable phases are identified with

Significance

The art of making structural, polymeric, and metallic glasses is rapidly developing with many applications. A limitation is that, under increasing external strain, all amorphous solids have a yield stress, which when exceeded, results in a plastic response leading to mechanical failure. Understanding this is crucial for assessing the risk of failure of glassy materials under loads. The universality of the mechanical yield requires a theory that is general enough to transcend the microscopic details of different glasses, which all show similar stress–strain curves with a yield point. We provide a general theory that is thermodynamic in nature, showing that the mechanical yield is a spinodal criticality in an appropriately constructed free energy landscape.

Author contributions: G.P., I.P., and C.R. designed research; I.P., C.R., and M.S. performed research; I.P., C.R., and M.S. analyzed data; and I.P. and C.R. wrote the paper.

Reviewers: A.C., Napoli University Federico II; and O.D., École Supérieure de Physique et de Chimie Industrielles de la Ville de Paris.

The authors declare no conflict of interest.

[1]To whom correspondence may be addressed. Email: giorgio.parisi@roma1.infn.it or Itamar.Procaccia@gmail.com.

This article contains supporting information online at www.pnas.org/lookup/suppl/doi:10.1073/pnas.1700075114/-/DCSupplemental.

its points of minimum in ϕ, and phase transitions happen when the curvature of these minima goes to zero, inducing a critical behavior that manifests diverging susceptibilities–fluctuations, critical slowing down of the dynamics, and growing correlation lengths (24). At a spinodal point, for example, one such minimum becomes unstable and transforms into a saddle. In the case of the order parameter Q_{ab}, the general form of the free energy $s[Q_{ab}]$ had been already derived and studied (ref. 25 has a review) in the context of the theory of replicas originally developed for the study of spin glasses, and its properties, at least at mean field level, are well-known (we refer to refs. 18 and 26 for the derivation of $s[Q_{ab}]$ in the specific case of mean field hard spheres); the matrix of second derivatives (or using a more field-theoretic terminology, the mass matrix) is not diagonal in the base of Q_{ab} and after diagonalization, is found to have only three distinct modes or masses (25). Of these masses, the most relevant ones are the so-called replicon mode λ_R, which for example, goes to zero at the newly proposed Gardner transition (27), and the longitudinal mode λ_L, which is, instead, related to spinodal points (18, 19), such as our yielding transition. In *SI Text*, we review briefly the background theory that is at the basis of this approach.

In this paper, we build up from the results of ref. 17, and following the line of reasoning formulated above, we use the expression of the correlation function relative to the longitudinal mode λ_L as it can be derived from the replicated field theory (25) to reveal the critical features of the yielding transition. We measure this correlator in numerical simulation and use it to expose the critical properties of the yielding transition, showing how shear bands manifest the diverging correlation length encoded in this correlator. We show how the order parameter Q_{ab} and its associated replicated field theory are thereby able to provide a unified and universal picture of the yielding transition in terms of a spinodal point in the presence of disorder, with an associated criticality.

Correlation Functions

The relevant order parameter for the problem at hand is the overlap function Q_{ab}, which measures the distance between two configurations a and b of the same system. Denoting the position of the ith particle as $\mathbf{r}_i^a$ in configuration a and $\mathbf{r}_i^b$ in configuration b, we define

$$Q_{ab} \equiv \frac{1}{N}\sum_{i=1}^{N}\theta(\ell - |\mathbf{r}_i^a - \mathbf{r}_i^b|), \qquad [1]$$

where $\theta(x)$ is the Heaviside step function, and ℓ is a constant length, which is taken below to be 1/3 in Lennard–Jones units (numerical details are given below). Thus, $Q_{ab}=1$ for two identical configurations, and $Q_{ab}=0$ when the distance between the positions of all of the particles i in the two configurations exceeds ℓ. Based on the introductory discussion, we now derive an expression for the correlator associated with the longitudinal mode, from whence one can extract the correlation length associated with the onset of criticality at the yielding point and define an associated susceptibility, which will shoot up as the yielding point is approached. The first step is to "localize" the overlap function and define the r-dependent quantity

$$Q_{ab}(\mathbf{r}) \equiv \sum_{i=1}^{N}\theta(\ell - |\mathbf{r}_i^a - \mathbf{r}_i^b|)\delta(\mathbf{r} - \mathbf{r}_i^a). \qquad [2]$$

Next, as mentioned above, the expression for the longitudinal correlator in terms of four-replica correlation functions can be found by diagonalization of the correlation matrix $G_{ab;cd}$, which is defined as the inverse of the mass matrix $M_{ab;cd}$ of the replicated field theory of the overlap order parameter Q_{ab} (25). The derivation is a matter of standard diagonalization algebra, and

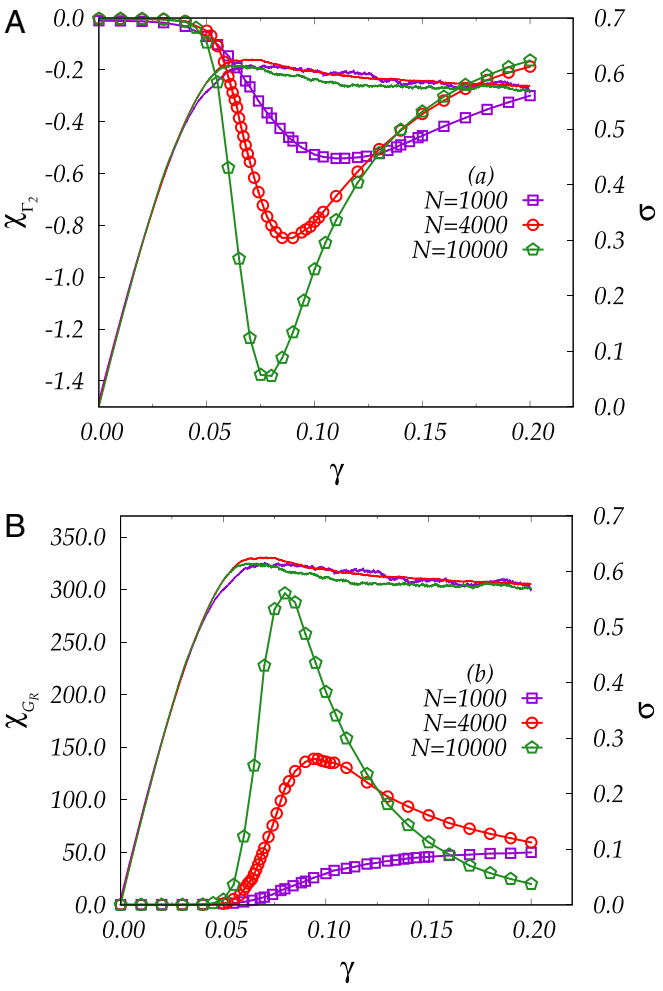

Fig. 1. The susceptibilities (*A*) χ_{Γ_2} and (*B*) χ_{G_R} as a function of γ for three systems sizes available. Superimposed are the stress versus strain curves for comparison. The color code is violet for $N=1{,}000$, red for $N=4{,}000$ and green for $N=10{,}000$.

therefore, we shall not report it here and refer to *SI Text* for the details. The expression, used, for example, in refs. 28 and 29 in the case of a model with spins on a lattice, reads for athermal systems

$$G_L(\mathbf{r}) = 2G_R(\mathbf{r}) - \Gamma_2(\mathbf{r}), \qquad [3]$$

with the definitions

$$G_R(\mathbf{r}) \equiv \overline{\langle Q_{ab}(r)Q_{ab}(0)\rangle} - 2\overline{\langle Q_{ab}(r)Q_{ac}(0)\rangle} + \overline{\langle Q_{ab}(r)\rangle\langle Q_{cd}(0)\rangle}, \qquad [4]$$

$$\Gamma_2(\mathbf{r}) \equiv \overline{\langle Q_{ab}(\mathbf{r})Q_{ab}(0)\rangle - \langle Q_{ab}(\mathbf{r})\rangle\langle Q_{ab}(0)\rangle}. \qquad [5]$$

Here, angular brackets denote a thermal average in the thermal case and an evaluation in an inherent state in the athermal case; an $\overline{(\bullet)}$ indicates an average over different samples of the glass. The quantity $G_R(r)$ is the correlation function of the replicon mode (25), and $\Gamma_2(r)$ is just the garden variety four-point correlator.

Using these definitions and taking Eq. **2** into account, the quantities that we compute in numerical simulation, before taking the ensemble average, are (*SI Text*) (30)

$$\tilde{\Gamma}_2(\mathbf{r}) = \frac{\sum_{i\neq j}(u_i^{ab} - Q_{ab})(u_j^{ab} - Q_{ab})\delta(\mathbf{r} - (\mathbf{r}_i^a - \mathbf{r}_j^a))}{\sum_{i\neq j}\delta(\mathbf{r} - (\mathbf{r}_i^a - \mathbf{r}_j^a))} \qquad [6]$$

and

$$\tilde{G}_R(\mathbf{r}) = \frac{\sum_{i\neq j}[u_i^{ab}u_j^{ab} - 2u_i^{ab}u_j^{ac} + Q_{ab}\ Q_{cd}]\delta(\mathbf{r} - (\mathbf{r}_i^a - \mathbf{r}_j^a))}{\sum_{i\neq j}\delta(\mathbf{r} - (\mathbf{r}_i^a - \mathbf{r}_j^a))} \quad [7]$$

with

$$u_i^{ab} \equiv \theta(\ell - |\mathbf{r}_i^a - \mathbf{r}_i^b|). \quad [8]$$

These four-replica objects can be computed for any quadruplet of distinct replicas. The ensemble averaged correlation functions are simply obtained as $\Gamma_2 \equiv \overline{\tilde{\Gamma}_2}$ and $G_R \equiv \overline{\tilde{G}_R}$ (compare with *SI Text* for a proof). We stress that one must keep the full space dependence of the correlators in the definitions above, because the introduction of shear breaks the rotational symmetry of the glass samples, and therefore, the correlators are not just functions of a distance r.

Numerics

To measure the quantities defined above, we performed molecular dynamics simulations of a Kob–Andersen 65–35% Lennard–Jones Binary Mixture in $2d$. We have three system sizes: $N = 1{,}000$, $N = 4{,}000$, and $N = 10{,}000$. We chose Q_{12} with $\ell = 0.3$ in Lennard-Jones units but verified that changes in ℓ leave the emerging picture invariant.

Following the procedure reported in ref. 17, as a first step, we prepared a glass by equilibrating the system at $T = 0.4$ and then quenching it (the rate is 10^{-6}) down to $T = 1 \cdot 10^{-6}$ into a glassy configuration. The sample is then heated up again to $T = 0.2$, and a starting configuration of particle positions is chosen at this temperature. Note that, whereas at $T = 0.4$, equilibration is sufficiently fast, at $T = 0.2$, the computation time is much shorter than the relaxation time. The configuration is then assigned a set of velocities randomly drawn from the Maxwell–Boltzmann distribution at $T = 0.2$, and these different samples are then quenched down to $T = 0$ at a rate of 0.1. This procedure can be repeated any number of times (say 100 times), and it allows us to get a sampling of the configurations, or replicas, inside one single "glassy patch." We then perform this procedure again, each time using a different configuration from the parent melt at $T = 0.4$, and in doing so, we get an ensemble of these glassy patches, each of them representing a distinct glass sample. For each of these patches, we measure the four-replica correlators defined above for any distinct quadruplet of replicas, averaging the result over any possible permutations of the quadruplet to gain statistics (29). The ensemble average is then performed by averaging the result over all of the glass samples. To perform these measurement, below, we use 100 patches for $N = 1{,}000$ (each with 100

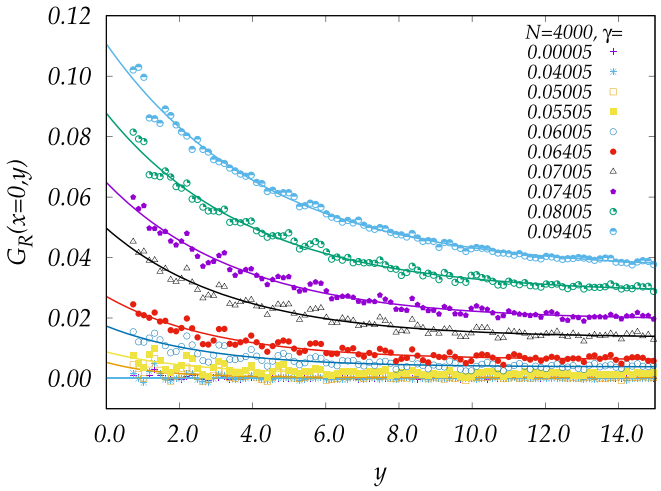

Fig. 2. The function $G_R(x = 0, y;\gamma)$ for various values of γ from 5×10^{-5} to 0.09405. Note the increase in the overall amplitude of the correlator as well as the increase in the correlation length. The lines through the data are the fit function **10**.

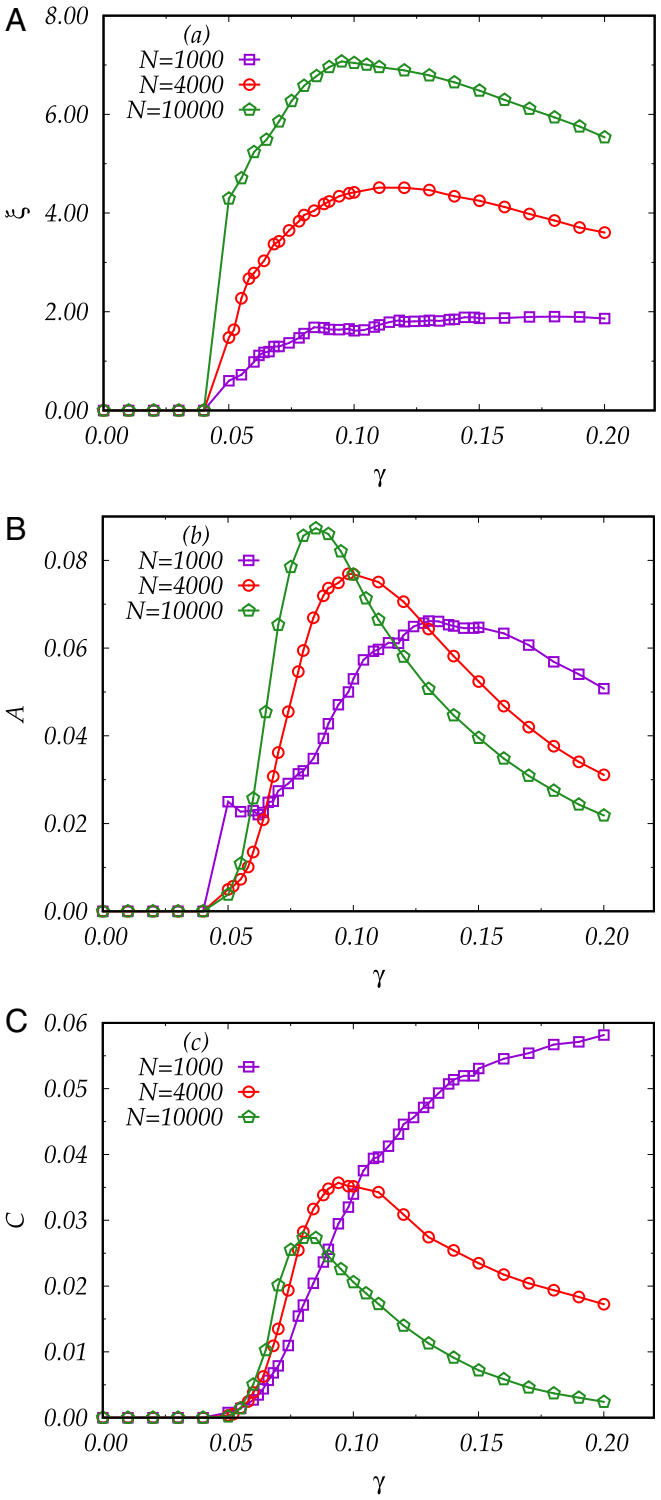

Fig. 3. The γ dependence of the correlation length $\xi(\gamma)$ (*A*), the amplitude $A(\gamma)$ (*B*), and the constant $C(\gamma)$ (*C*) in the best fit to the function $G_R(x = 0, y; \gamma)$ (compare with **10**).

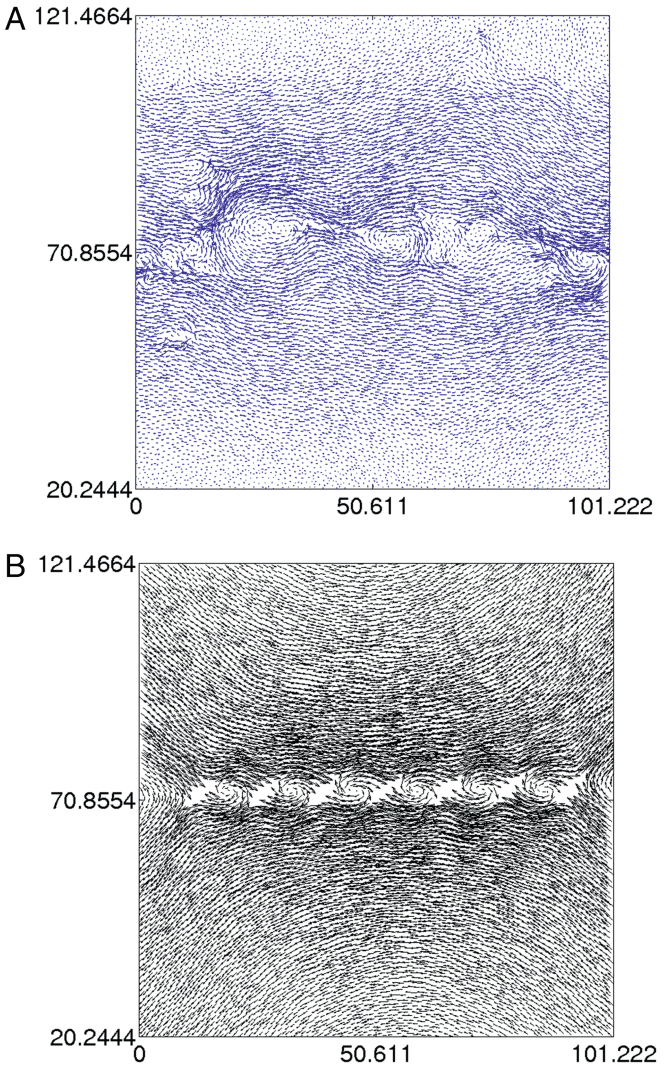

Fig. 4. Example of the spontaneous plastic event exhibiting a concatenation of a series of Eshelby quadrupoles resulting in a correlated displacement field with shear localization over a thin region, which is system-spanning. (*A*) Direct numerical simulations. (*B*) Inserted line of Eshelby quadrupoles.

configurations), 100 patches for $N = 4{,}000$ (each with 50 configurations), and 50 patches for $N = 10{,}000$ (each with 50 configurations). A strain γ_{xy} (denoted below as γ) is then applied quasistatically to all configurations in all patches. In this protocol, after every step of increased strain, the system undergoes energy gradient minimization to return to mechanical equilibrium. This procedure creates an ensemble of strained patches for every value of the strain parameter γ, from whence we measure again the above defined correlators, which then become functions of the strain γ. This behavior is simply a consequence of the response of the configurations [i.e., each position $\mathbf{r}_i$ in the definitions above becomes $\mathbf{r}_i(\gamma)$]. Thus, for example, $G_R(r)$ becomes $G_R(r;\gamma)$, etc. We are interested in the behavior of the correlators as the yielding point γ_Y is approached.

Results

We consider first the susceptibilities χ_{G_L}, χ_{G_R} and χ_{Γ_2} that can be obtained from the correlators; for example,

$$\chi_{G_L}(\gamma) \equiv \int d^2x\; G_L(x,y;\gamma). \qquad [9]$$

In Fig. 1, *Upper*, we show the susceptibility χ_{Γ_2} as a function of γ for three system sizes at our disposal. Superimposed are the stress versus strain curves obtained by averaging the individual curves over all of the available configurations and glass samples. One sees very clearly the singularity that develops near the yield point as a function of the system size. In Fig. 1, *Lower*, we show the susceptibility χ_{G_R} as a function of the strain γ, again with the stress–strain curve superimposed for comparison. As we expected, the susceptibilities show a distinct peak at the spinodal point γ_Y, wherein yielding occurs. Because χ_{Γ_2} is much smaller in amplitude than χ_{G_R}, there is not much new information in χ_{G_L}, which is $\sim 2\chi_{G_R}$.

More detailed information is provided by the full dependence of the correlators on their arguments. To see most clearly the change in the correlators as the spinodal point is approached, it is best to consider, for example, the 1D function $G_R(x=0,y;\gamma)$, shown for $N = 4{,}000$ in Fig. 2. Similar results for the other systems sizes are available in *SI Text*. We note that the correlator changes in both amplitude and extent when we approach the critical point. To quantify these changes, we fit a three-parameter function to $G_R(x=0,y)$ in the form

$$G_R(x=0,y;\gamma) \approx C + A\exp\left(-\frac{y}{\xi}\right), \qquad [10]$$

where all of the fitting coefficients are functions of γ. In Fig. 3, we present the γ dependence of the amplitude $A(\gamma)$, the constant $C(\gamma)$, and the correlation length $\xi(\gamma)$.

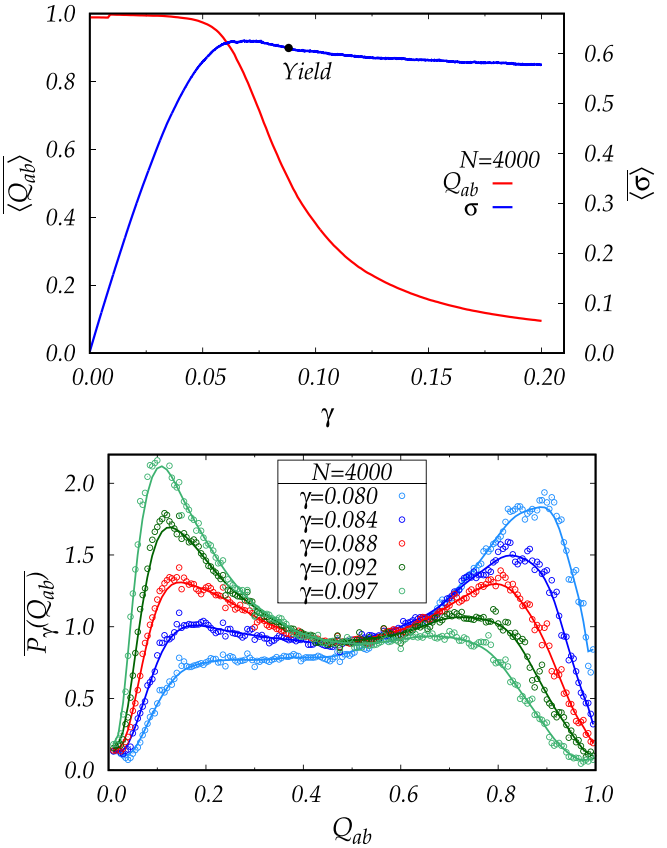

Fig. 5. (*Upper*) The order parameter $\overline{Q_{ab}}$ as a function of the strain γ superimposed on the stress versus strain curve. (*Lower*) The probability distribution function $P(\overline{Q_{ab}})$ for different values of γ in the vicinity of the mechanical yield value γ_Y.

It is interesting to notice that the constant C decreases with the system size, presumably becoming irrelevant in the thermodynamic limit. The amplitude A is still increasing with the system size, and it is difficult to assert whether it converges or not. However, we can safely conclude that the data present a strong evidence for the increase in the correlation length; it is very likely that it should diverge in the thermodynamic limit.

Relevant questions are whether one can define critical exponents that can also be measured in experimental situations and whether such exponents can be computed from theory, even on the mean field level. Clearly, the standard thermal mean field approach cannot be used, because averages here are computed over replicas at $T = 0$, and fluctuations caused by quenched disorder are expected to dominate the thermal fluctuations that stem only from the mother supercooled liquid from which the replicas at $T = 0$ are created. Considerations of the effect of such fluctuations are beyond the scope of this paper and will be discussed elsewhere.

Physical Interpretation

To conclude this paper, we present a physical interpretation to these insights, connecting them to what is known about the mechanical yield in athermal amorphous solids. The most important characteristic of the mechanical yield in athermal amorphous solids is the change from plastic responses that are localized, typically in the form of Eshelby quadrupoles, to subextensive plastic events that are system-spanning (31, 32). The energy drops associated with the localized Eshelby quadrupoles are system size-independent, scaling like N^0, where N is the total number of particles in the system. Mechanical yield is associated with the spontaneous appearance of concatenated lines of quadrupoles [in two dimensions or planes in three dimensions (13, 15, 16)]. The latter are associated with energy drops that are subextensive, scaling like $N^{1/3}$ in two dimensions. Importantly, the concatenated lines of quadrupoles change drastically the displacement field associated with the plastic events. Each quadrupole has an arm with a displacement field pointing outward and an arm with the displacement field pointing inward. When the quadrupole is isolated, the displacement field decays algebraically to infinity. In contrast, when the quadrupoles are organized in the line, there is a global connection between the outgoing direction of one quadrupole and the incoming direction of the next, making the displacement field strongly localized around the line of quadrupoles (or around a plane in three dimensions), and all of the shear is there. This excitation is a microscopic shear band. An example of the displacement field associated with such a system-spanning event is shown in Fig. 4 (details are in ref. 13). The main point of this paper is that the highly correlated phenomenon of such a shear band can only occur when there exists a correlation length that approaches the system size in magnitude. This length is the correlation length ξ that is identified in this paper (compare with Fig. 3, *Top*).

To understand the relevance of the spinodal point for this scenario, we provide two figures that were obtained in ref. 17. In Fig. 5, *Upper*, one sees the order parameter Q_{ab} as a function of γ superimposed on the stress versus strain curve of the system under study. The point "yield" was obtained with the help of the results shown in Fig. 5, *Lower*, in which the probability of observing Q_{ab} is plotted for values of γ around the mechanical yield point γ_Y. The yield itself is identified when the probability distribution function has two peaks of the same height. The spinodal point is at a slightly higher value of γ, where the peak occurring around high values of Q_{ab} is about to disappear, with a characteristic spinodal vanishing of the slope. This spinodal is occurring in this system around $\gamma = 0.1$. Of course, in the thermodynamic limit, the whole range of γ values where the exchange of stability is occurring is becoming very narrow.

It is important to stress again that the ability to observe the divergence of the susceptibility and the correlation length caused by the spinodal phenomenon stems from the fact that we deal with an athermal glassy system with typical relaxation times that are immense. In a liquid system, the fluctuations would have caused the system to make the transition before the spinodal point is reached.

Conclusions

In conclusion, we have presented evidence that the yielding transition is a spinodal point with disorder characterized by a criticality with features that can be picked up by suitable multipoint correlators, with expression that can be obtained from replica theory. The treatment presented here pertains to an athermal setting, but an obvious direction for future research will be the application of these ideas to thermal glasses under shear (21); in the finite temperature case, the system will generally be able to escape through thermal activation from the high-Q_{ab} minimum before this has a chance to flatten and the relative susceptibility to diverge. However, because the nucleation time will anyway be fairly long, one should anyway be able to observe transient shear bands/heterogeneities as long as the temperature is low enough that nucleation does not take place until the system is close to the spinodal, which interestingly, is precisely the behavior of transient shear bands as reported in ref. 21. In this thermal setting, we expect that the study of the ideas presented in this paper will have to proceed much as it does in the case of dynamical heterogeneities around the mode coupling cross-over, entailing, for example, the definition and study of time-dependent multipoint susceptibilities and correlators.

ACKNOWLEDGMENTS. We thank George Hentschel and Francesco Zamponi for inspiring discussions. G.P. acknowledges funding from the European Research Council under European Union's Horizon 2020 Research and Innovation Program Grant 694925. I.P. was supported, in part, by the Minerva Foundation with funding from the Federal German Ministry for Education and Research and the Israel Science Foundation (Israel Singapore Program). I.P. acknowledges receiving the Premio Rita Levi-Montalcini, which facilitated the collaboration with G.P.

1. Landau LD, Lifshitz EM (1959) *Course of Theoretical Physics Vol. 7: Theory of Elasticity* (Pergamon, Oxford).
2. Varnik F, Bocquet L, Barrat J-L (2004) A study of the static yield stress in a binary lennard-jones glass. *J Chem Phys* 120:2788–2801.
3. Maloney C, Lemaître A (2004) Subextensive scaling in the athermal, quasistatic limit of amorphous matter in plastic shear flow. *Phys Rev Lett* 93:016001.
4. Demkowicz MJ, Argon A (2005) Liquidlike atomic environments act as plasticity carriers in amorphous silicon. *Phys Rev B* 72:245205.
5. Tanguy A, Leonforte F, Barrat J-L (2006) Plastic response of a 2d lennard-jones amorphous solid: Detailed analysis of the local rearrangements at very slow strain rate. *Eur Phys J E Soft Matter* 20:355–364.
6. Lemaître A, Maloney C (2006) Sum rules for the quasi-static and visco-elastic response of disordered solids at zero temperature. *J Stat Phys* 123:415–453.
7. Lerner E, Procaccia I (2009) Locality and nonlocality in elastoplastic responses of amorphous solids. *Phys Rev E* 79:066109.
8. Rodney D, Tanguy A, Vandembroucq D (2011) Modeling the mechanics of amorphous solids at different length scale and time scale. *Model Simul Mat Sci Eng* 19:083001.
9. Subhash G, Liu Q, Gao X-L (2006) Quasistatic and high strain rate uniaxial compressive response of polymeric structural foams. *Int J Impact Eng* 32:1113–1126.
10. Kara A, Tasdemirci A, Guden M (2013) Modeling quasi-static and high strain rate deformation and failure behavior of a ($\pm$45) symmetric e-glass/polyester composite under compressive loading. *Mater Des* 49:566–574.
11. Noradila AL, Sajuri Z, Syarif J, Miyashita Y, Mutoh Y (2013) Effect of strain rates on tensile and work hardening properties for al-zn magnesium alloys. *IOP Conference Series: Materials Science and Engineering*, eds Gaol FL, Hussain RR, Pandiangan T, Desai A (IOP Publishing, Bristol, UK), Vol 46, p 012031.
12. Berthier L, Biroli G (2011) Theoretical perspective on the glass transition and amorphous materials. *Rev Mod Phys* 83:587–645.
13. Dasgupta R, Hentschel HGE, Procaccia I (2012) Microscopic mechanism of shear bands in amorphous solids. *Phys Rev Lett* 109:255502.
14. Ashby MF, Greer AL (2006) Metallic glasses as structural materials. *Scr Mater* 54: 321–326.
15. Dasgupta R, Hentschel HGE, Procaccia I (2013) Yield strain in shear banding amorphous solids. *Phys Rev E* 87:022810.

16. Dasgupta R, Gendelman O, Mishra P, Procaccia I, Shor CABZ (2013) Shear localization in three-dimensional amorphous solids. *Phys Rev E* 88:032401.
17. Jaiswal PK, Procaccia I, Rainone C, Singh M (2016) Mechanical yield in amorphous solids: A first-order phase transition. *Phys Rev Lett* 116:085501.
18. Rainone C, Urbani P (2016) Following the evolution of glassy states under external perturbations: The full replica symmetry breaking solution. *J Stat Mech Theor Exp* 2016:053302.
19. Urbani P, Zamponi F (2017) Shear yielding and shear jamming of dense hard sphere glasses. *Phys Rev Lett* 118:038001.
20. Nandi SK, Biroli G, Tarjus G (2016) Spinodals with disorder: From avalanches in random magnets to glassy dynamics. *Phys Rev Lett* 116:145701.
21. Shrivastav GP, Chaudhuri P, Horbach J (2016) Heterogeneous dynamics during yielding of glasses: Effect of aging. *J Rheol (N Y N Y)* 60:835–847.
22. Regev I, Lookman T (2017) The irreversibility transition in amorphous solids under periodic shear. *Avalanches in Functional Materials and Geophysics*, eds Abarbanel H, Braha D, Érdi P, Friston K, Haken H, Jirsa V, Kacprzyk J, Kaneko K, Kelso S, Kirkilionis M, Kurths J, Menezes R, Nowak A, Qudrat-Ullah H, Reichl L, Schuster P, Schweitzer F, Sornette D, Thurner S (Springer, Berlin), pp 227–259.
23. Leishangthem P, Parmar ADS, Sastry S (2017) The yielding transition in amorphous solids under oscillatory shear deformation. *Nat Commun* 8:14653.
24. Zinn-Justin J (2002) *Quantum Field Theory and Critical Phenomena* (Oxford Univ Press, Oxford).
25. de Dominicis C, Kondor I, Temesvári T (1998) Beyond the Sherrington-Kirkpatrick model. *Spin Glasses and Random Fields*, ed Young AP (World Scientific, Singapore), pp 119–160.
26. Rainone C, Urbani P, Yoshino H, Zamponi F (2015) Following the evolution of hard sphere glasses in infinite dimensions under external perturbations: Compression and shear strain. *Phys Rev Lett* 114:015701.
27. Charbonneau P, Kurchan J, Parisi G, Urbani P, Zamponi F (2014) Fractal free energy landscapes in structural glasses. *Nat Commun* 5:3725.
28. Baity-Jesi M, et al. (2014) The three-dimensional ising spin glass in an external magnetic field: The role of the silent majority. *J Stat Mech Theor Exp* 2014: P05014.
29. Baity-Jesi M, et al. (2014) Dynamical transition in the $d = 3$ edwards-anderson spin glass in an external magnetic field. *Phys Rev E* 89:032140.
30. Berthier L, et al. (2016) Growing timescales and lengthscales characterizing vibrations of amorphous solids. *Proc Natl Acad Sci USA* 113:8397–8401.
31. Karmakar S, Lerner E, Procaccia I (2010) Athermal nonlinear elastic constants of amorphous solids. *Phys Rev E* 82:026105.
32. Gendelman O, Jaiswal PK, Procaccia I, Gupta BS, Zylberg J (2015) Shear transformation zones: State determined or protocol dependent? *Europhys Lett* 109: 16002.
33. Franz S, Parisi G (1995) Recipes for metastable states in spin glasses. *J Phys I* 5: 1401–1415.
34. Bender CM, Orszag SA (1999) *Advanced Mathematical Methods for Scientists and Engineers I* (Springer Science & Business Media, Berlin).
35. Rainone C (2014) The replica method in liquid theory: From the basics to explicit computations. arXiv:1411.3941.
36. Kurchan J, Parisi G, Zamponi F (2012) Exact theory of dense amorphous hard spheres in high dimension I. The free energy. *J Stat Mech Theor Exp* 2012: P10012.
37. Crisanti A, Sommers H-J (1992) The spherical p-spin interaction spin glass model: The statics. *Zeitschrift für Physik B* 87:341–354.
38. Bray AJ, Moore MA (1979) Replica symmetry and massless modes in the ising spin glass. *J Phys C Solid State Phys* 12:79–104.
39. Zamponi F (2010) Mean field theory of spin glasses. arXIV:1008.4844.